Development of New Field Testing Tools for Geothermal Power Plant Risk Assessment of Corrosion and Scaling

Kazumi Osato[1], Masatake Sato[1], Kaichiro Kasai[1], Mikio Omae[1],

Norio Yanagisawa[2], Koji Sakura[3], and Keith Lichti[4]

[1]Geothermal Energy Research and Development Co., Ltd., Shinkawa-1 Chome 22-4, Cyuo-ku, Tokyo 104-0033, Japan

[2] Renewable Energy Research Center, AIST, 2-2-9, Machiikedai, Koriyama, Fukushima 963-0298, Japan

[3]TenarisNKKTubes K. K., 1-10, Minamiwatarida, Kawasaki, Kanagawa, 210-0855, Japan

[4]Quest Integrity NZ Ltd., 69 Gracefield Road, Lower Hutt, Lower Hutt 5045, New Zealand

osato@gerd.co.jp

Keywords: *Corrosion, Scaling, Field Testing, Geothermal*

ABSTRACT

We are developing two field testing tools for geothermal power plant risk assessment of corrosion and scaling under NEDO's "Research and Development of Geothermal Power Generation Technology Program". The first tool is the portable flow loop corrosion tester. The second one is the Gamma-ray pipe section profiler to measure the scale blockage rate of piping. We are developing the portable flow loop corrosion tester using 1" piping for geothermal single and two-phase flow condition. This tester can be easy to handle by a few workers without a crane and is low cost. The tester can be set up for three corrosion rate measurement methods – ER(Electrical Resistance) Corrosometer®, LPR (Linear Polarization Resistance), and Cylinder coupon exposure tests. The tester can also be set up for any injection systems of acids (H_2SO_4, HCl, to simulate extreme acidic condition), NaOH (for neutralization) or anti-corrosion/anti-scalant inhibitors. We have already trialed this tester in liquid flow condition (Kakkonda, Iwate) and two-phase flow condition (Okuaizu, Fukushima) in 2016-2017. The basis of the gamma-ray pipe section profiler is to measure the difference of gamma-ray transmission of steel pipe, insulation, geothermal flow, and scale at pipe cross-sections. We have already trialed this profiler in a reinjection pipeline in Kakkonda steam field and a production pipeline in Okuaizu steam field and compared with visual observations during the regular inspection of each power plant in 2015-2017. This paper shows basis, summary of field tests, estimation of tool accuracy, and issues in the futures of these tools.

® Rohrback Cosasco Systems, Inc.

1. INTRODUCTION

Figure1 is the concept of the system to control corrosion & scale problems of geothermal fluid for wellbore and surface pipeline described by Sanada et al. (2000), Lichti et al. (1998 & 2005). Geothermal fluid has variable conditions changing pH or salinity and that has significant influence on the material selection of casing pipe and pipeline design. Previously, we obtained samples of fluid at the surface at room temperature and estimated the condition of borehole or surface pipeline. Our new approach is using pipe flow simulation to simulate the conditions of the wellbore or surface pipeline at first and to couple to chemical model in the second. Our chemical model can also calculate Pourbaix diagrams for corrosion and saturation index for scaling predictions (Osato et al., 2016).

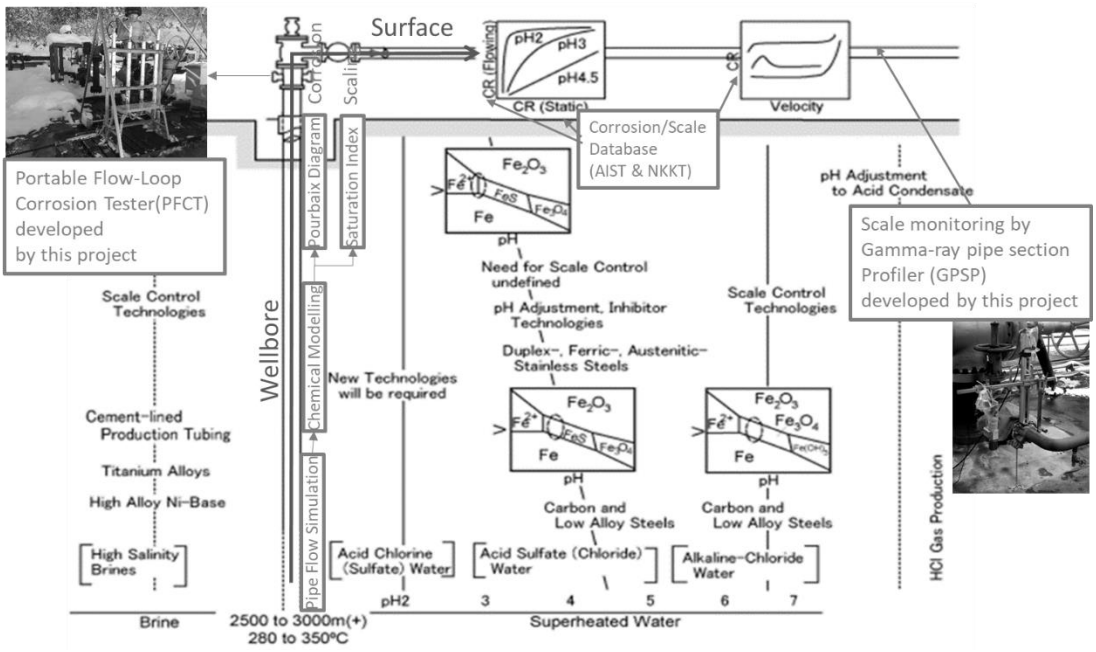

Figure 1: Concept to control corrosion & scale of geothermal fluid (Modified Sanada et al., 2000)

Also, we combined it with corrosion rate prediction method based on two approaches by AIST - Cr equivalent method (Yanagisawa et al., 2016) and NKKT - interpolation method using AIST's corrosion database that had been AIST-Tohoku branch's achievement of METI's Sunshine and New Sunshine Project from 1974 to 2002 (Sanada et al., 2000 & Yanagisawa et al., 2016). If the simulation duplicates the real phenomena referred by database and field test, we can predict the environment of wellbore and surface pipeline in several conditions by parameter study. Two field testing tools (Portable flow loop corrosion tester and Gamma-ray pipe section profiler) are being developed to achieve such purposes.

2. MECHANISM OF FIELDS TEST TOOLS

2.1 Portable flow loop corrosion tester (PFCT)

Since full size flow loop test needs real scale bypass pipeline taking along the commercial pipeline, it requires the following conditions;

1) Stop real pipe line and undertake large scale piping work.
2) Large flow rate has to bypass to the test line
3) Larger test coupons are required even if testing high grade materials.

Therefore, the test schedule cannot match in owner's good time and the test scale has to be larger and this drives up the cost.

Portable flow loop corrosion tester (PFCT) has been designed to simulate real scale pipeline flow condition using 1" OD small pipes with four Y-block ports that can measure the following data;

1) Electrical resistance (ER) probe :① of Figure 2
2) Linear polarization resistance (LPR) probe :② of Figure 2
3) Multiple test coupon (cylinder type) for material weight loss test in flow condition : ③ of Figure 2
4) Temperature, Pressure, pH and chemical sampling

Figure 2 is the schematic of PFCT tool. The tool is designed to lay down for liquid phase flow and set up vertically for two phase flow and steam flow because the LPR probe can only measure under conductive liquid phase condition. Since ② position (setting up vertically) can be filled by the liquid, LPR probe can contact to the liquid.

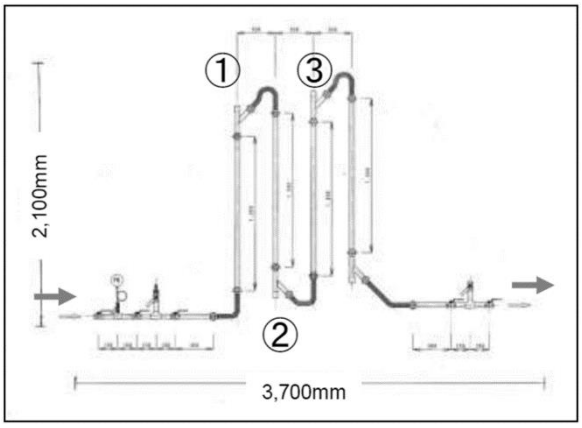

Figure 2: Schematic of Portable flow loop corrosion tester (PFCT)

CORROSOMETER® (ER probe) technology is based on the electrical resistance method of corrosion monitoring pioneered by Rohrback Cosasco in the 1950's and 1960's. The probes are basically "automatic coupons." They determine the loss of metal. from the probe by measuring the change in its resistance. Because of the very low resistances involved, very sensitive monitoring circuits are used in the instruments to measure the change in probe resistance compared to the resistance of a protected reference element connected in series to the corroding measurement element. A "check" element is also included and is protected from the process fluid along with the reference element. The ratio of check-to-reference resistance should remain constant. If it doesn't, this indicates that degradation of the reference element may be occurring due to perforation of the thin walled test element and that metal. loss readings obtained from the probe are questionable. A simplified diagram of a typical electrical resistance monitoring circuit is shown in Figure 3 (Rohrback Cosasco).

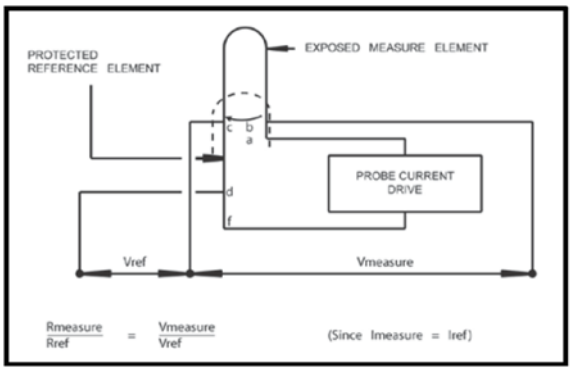

Figure 3: Simplified Electrical Resistance Monitoring Circuit (Rohrback Cosasco)

Electrical resistance (ER) probes (CORROSOMETER®) are available in a variety of styles and with useful probe life ("span") ranging from 2-25 mils in styles commonly used in process piping systems. Iinstrumentation to measure electrical resistance probes divides the probe span into 1000 "divisions." A probe with a 2 mil span is therefore theoretically capable of measuring thickness changes of 0.002 mils. In practice, for detection of corrosion upsets, Rohrback Cosasco generally recommends that a change in indicated metal. loss of 10 divisions or 1% of, and corrosion upset rate from background noise (Rohrback Cosasco).

Rohrback Cosasco's CORRATER® systems measure the instantaneous corrosion rate of a metal. in a conductive fluid using the DC linear polarization resistance (LPR) measurement technique. This technology only applies to conductive liquids (water) and is usually used to monitor corrosion rates in cooling water systems of all kinds. It provides the feedback for the chemical treatments being employed. Some instruments also include an AC measurement for correction of solution resistance. Stern and Geary originally demonstrated that the application of a small polarizing potential difference (ΔE) from the corrosion potential (E_{corr}) of a corroding electrode resulted in a measured current density (i_{meas}) which is related to the corrosion current density (i_{corr}) by equation (1).

$$\frac{\Delta E}{i_{meas}} = \frac{b_a b_c}{(2.303\, i_{corr})(b_a + b_c)} \qquad (1)$$

Here: b_a = Anodic Tafel Slope, b_c = Cathodic Tafel Slope

Since the Tafel coefficients are more or less constant for a given metal./fluid combination, i_{meas} is proportional to i_{corr} is proportional to the corrosion rate. Equation (1) and the entire

LPR technique are only valid when the polarizing potential difference is very low (typically up to 20 mV). In this region, the curves approach linearity, hence the term LPR. Inspection of equation (1) shows that the result $\Delta E/i_{meas}$ is a resistance term called, the Polarization Resistance, R_p. The resistance to current flow between electrodes of a two-electrode LPR probe is the sum of polarization resistance values at each electrode and the resistance of the solution between the electrodes (R_s) as shown in equation (2):

$$\Delta E = i_{meas}(2R_p + R_s) \qquad (2)$$

From equations (1) and (2), obtaining results from the LPR technique would seem to require only instantaneous readings of resistance. In practice, however, the determination of polarization resistance is complicated by a capacitance effect at the metal/fluid interface (double-layer capacitance). Figure 4 is an equivalent electrical circuit of the corrosion cell formed by the measuring electrodes and the fluid, showing the importance of R_s and double-layer capacitance effects (Rohrback Cosasco).

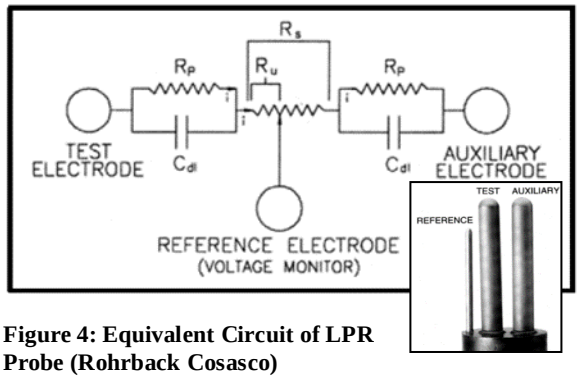

Figure 4: Equivalent Circuit of LPR Probe (Rohrback Cosasco)

The effect of the double-layer capacitance is to require the direct current flow to initially charge-up the capacitors to the polarization potential, resulting in a decaying exponential current flow curve vs. time, after application of the polarizing potential difference. The measurement tools provided by Rohrback Cosasco for LPR corrosion rate determination account for the effects of capacitance and solution resistance under extremes of low conductivity fluids and changing capacitance due to film formation. These effects can be sufficiently severe as to prevent the instruments ability to determine corrosion rate, however, the electrodes used for the testing are also used as weight loss coupons for comparison with the LPR determined rates.

Figure 6: Pictures of PFCT at Okuaizu in Feb. 2016

Figure 5: Pictures of PFCT at Kakkonda in Nov. 2015

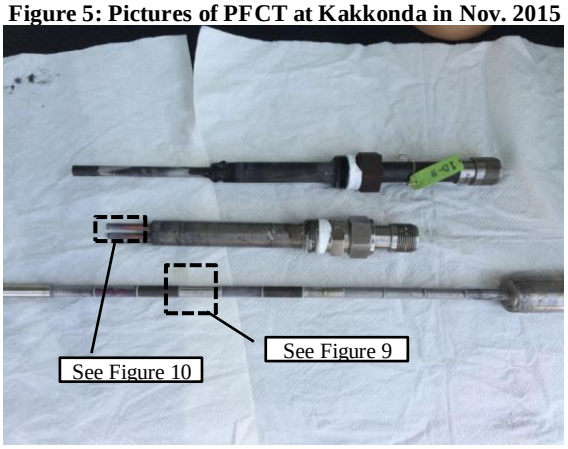

Figure 7: ER Probe, LPR Probe and Cylinder Coupon (from above)

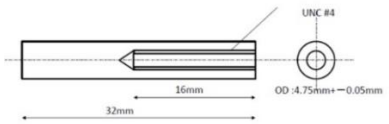

Figure 8 Schematic of Electrode for LPR probe

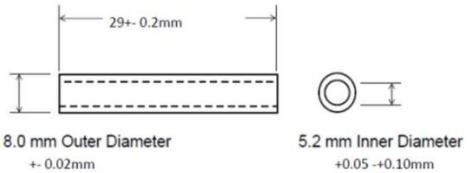

Figure 9 Schematic of Cylinder Coupon

2.2 Gamma-ray pipe section profiler (GPSP)

The scaling blockage of pipeline is not easy to find without removing pipes in sections that are flanged or welding cut. Therefore, the maintenance time of pipelines used to be presumed by their experience of pressure change in flow. Therefore, a pipe section profiler is a very efficient tool to determine the maintenance schedule of pipelines in the geothermal plants.

The gamma ray pipe section profiler (GPSP) is a kind of gamma ray transmission type density meter. It estimates the density of fluid from the degree of attenuation when gamma rays pass through the fluid in the pipe.

The density meter and gamma-ray source (its transport is legally permitted in Japan) is fixed in parallel by an arm that drives by an elevating motor clamped on the top of the piping, and it is arranged so that the isotope which is the gamma ray source (^{60}Co, 3.7MBq) and the scintillation detector (Thallium doped sodium iodide crystal 2x2 inch) face each other across the piping.

The source part in which the gamma ray source is stored is covered with a shield except for the direction of the detector, and radiation leaking to the outside through the shield is negligible. On the other hand, gamma rays directed towards the detector are shielded by the shielding ability of the detector itself and only a small amount of radiation leaks in that direction.

Key elements of the GPSP are illustrated in Figures 10 to 13.

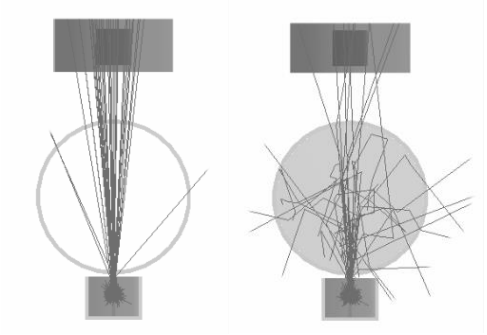

(i) Piping only (ii) Piping filled by water or scaling

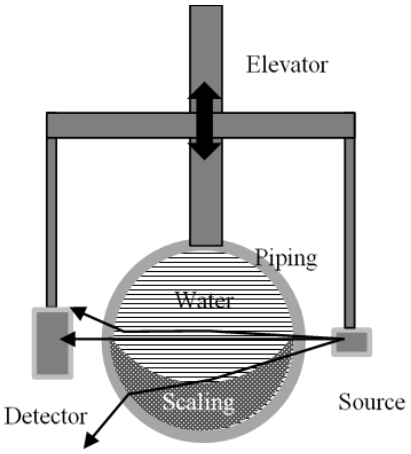

(iii) Developed system

Figure 10 Simplified mechanism of gamma-ray absorption and scattering due to inner pipe materials (water and scaling) between a source and a detector

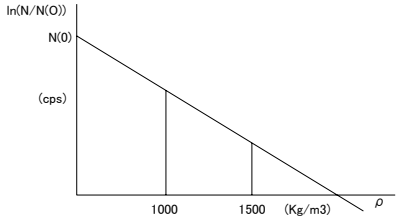

Figure11 Relationship between counting rate and density

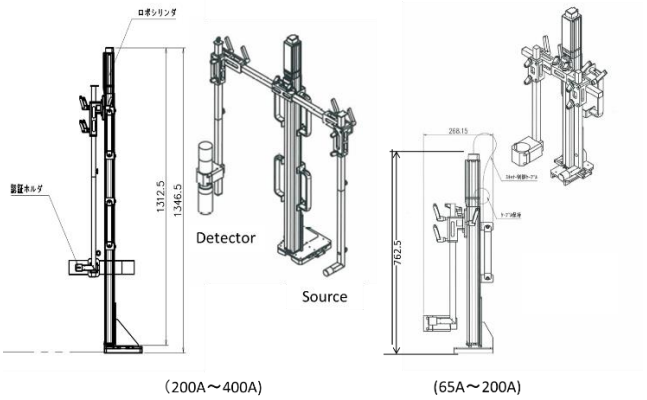

Figure 12 Sketch of gamma ray pipe section profiler

Figure 13 Setting up of Gamma-ray pipe section profiler (GPSP) in the field

3. FIELD TEST RESULTS

3.1 Portable flow loop corrosion tester (PFCT)

In 2015 -2017, we have tried to apply PFCT once in Kakkonda steam field (liquid phase flow) and twice in Okuaizu steam field (two phase flow) given in Table 1;

Table 1. Field tests in 2015 -2017

Field name	M/Y (days)	Phase	P,T,V	pH
Kakkonda	Nov.2015 (5days)	Liq.	120-145℃ 0.17-0.32MPa 344-620kg/h	3.6
Okuaizu1	Jan. 2016 (3 days)	2 ϕ	163-168℃ 0.66-0.68MPa 240-438kg/h	4.9
Okuaizu2	Feb. 2017 (26 days)	2 ϕ	168-173℃ 0.75-0.76MPa 270-288kg/h	3.8 & 3*

*: pH control by adjunction of HCl or H_2SO_4 at upstream

Test materials: K55 (Carbon Steel), TN80SS(1%Cr), TN80Cr13(13%Cr), TN110Cr13S(13%Cr+1%Mo), SAF 2507 (Duplex) in all fields (samples provided by NKKT) and optionally Titanium (Grade12) (samples provided by TIMET) in Okuaizu2

Table 2 gives extrapolated Corrosometer® result in Kakkonda tests. The testing was made in 6 exposure conditions. Figure 14 is example of material loss curves vs. exposure time of TEST4. We estimated the material loss of carbon steel = 0.042 mm/yr by 1,380 minutes of measurement. Figure 15 shows the surface of Corrosometer® electrode after test.

Table 2 Kakkonda: Corrosometer® for carbon steel (CS)

Test ID	Material	Exposure Time (minutes)	Material loss(mm/yr)	P (MPa)	T (℃)	Velocity (m/s)	pH
TEST1	CS	155	0.426	0.20	132	0.25	3.6
TEST2	CS	150	0.240	0.30	145	0.19	3.6
TEST3	CS	1038	0.040	0.22	135	0.25	3.6
TEST4	CS	1380	0.042	0.32	145	0.31	3.6
TEST5	CS	1410	0.104	0.24	135	0.33	3.6
TEST6	CS	120	3.132	0.17	120	0.34	3.6

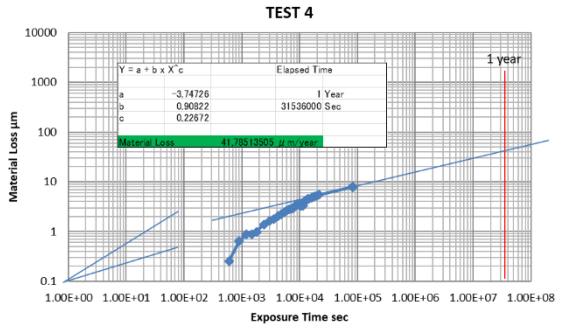

Figure 14 Kakkonda: Corrosometer® curve of TEST4 and prediction of material loss per year

Figure 15 Kakkonda: The surface of Corrosometer® Probes (CS, SS) and LPR electrodes after testing

Figure 16 shows all of Corrosometer® curves for Kakkonda field testing obtained using PFCT. The variation in the data was not so large.

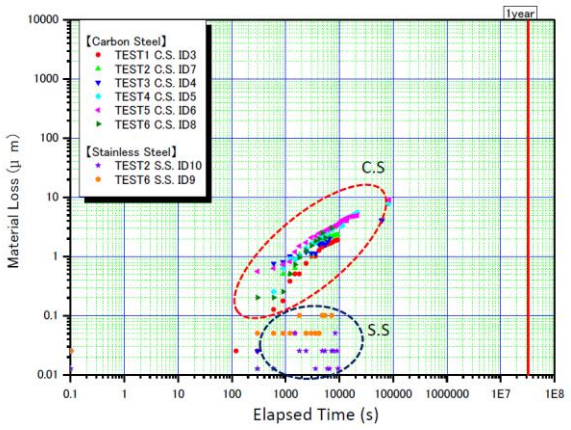

Figure 16 Kakkonda: Corrosometer® plot of all tests (material: CS and SS)

Table 3 gives Corrosometer® result in Okuaizu1 tests with the PFTC.The testing was made in 6 exposure conditions. In these condition, carbon steel had negligible material loss (all less than 0.006mm/yr).

Table 3 Okuaizu1: Corrosometer® for carbon steel (CS) and stainless steel (SS)

Test ID	Material	Exposure Time (minutes)	Material loss(mm/yr)	P (MPa)	T (℃)	Velocity (m/s)	pH
TEST1	CS	80	0.006	0.66	163	6.0	4.9
TEST2	CS	115	0.001	0.68	168	4.0	4.9
TEST3	CS	1295	0.001	0.66	133	6.7	4.9
TEST4	CS	1075	0.001	0.68	168	4.0	4.9
TEST5	CS	1030	0.000	0.66	164	7.3	4.9
TEST6	CS	145	0.000	0.66	163	6.8	4.9
TEST2	SS	115	0.000	0.68	168	4.0	4.9

Figure 17 Okuaizu1: The surface of Corrosometer® Probes (CS) after testing

Figure 17 illustrates the appearance of the Corrosometer® probes after testing while. Figure 18 shows all of Corrosometer® curves for Okuaizu1 field test. Since the material loss was very small, the variation in the data was range that could be ignored.

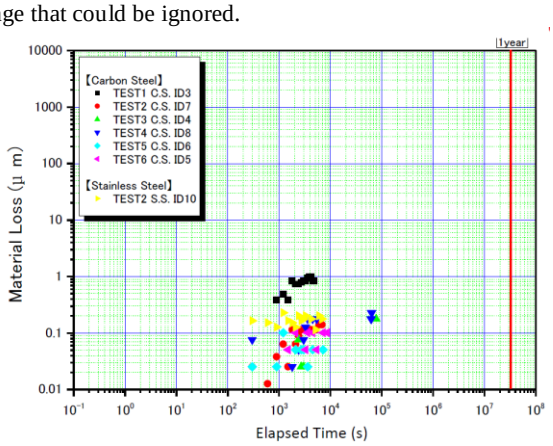

Figure 18 Okuaizu1: Corrosometer® plot of all tests (material: CS and SS)

Table 4 gives the weight loss test results obtained using cylinder coupons at Kakkonda. Figure 19 shows an example of the cylinder coupon string which had been inserted into PFCT in Kakkonda. All coupons are skewered with a Teflon covered metallic stick and each cylinder coupon is isolated electrically from other coupons on both sides by Teflon sleeve. If we need to test bimetallic corrosion, we can take out a sleeve which is normally used to isolated target materials.

Table 5 is the weight loss test result using cylinder coupon in Okuaizu1.

We could measure small weight loss in short time test in both fields.

The results of Kakkonda field test are summarized as follows;

1) Result of long term test coupons; there are black deposit on K-55 and TN80SS. We observed a colour change on TN80Cr13, but there was only a small amount of deposit. TN110Cr13S showed no deposit on the material.

Table 4 Kakkonda: Weight loss test using cylinder coupon

Material	Test ID	Initial Weight (g)	After Exposure (g)	Difference (g)	Difference After DHACP (g)	Exposure Time (h)	Specific Weight	O.D (mm)	I.D (mm)	Length (mm)	Area (mm2)	Volume (mm3)	Calculated Weight (g)	Corrosion Thickness (mm)	C.R. (mm/y)	C.R. Average (mm/y)
K-55	TEST -4 RP1	6.4553	6.4482	-0.0071	0.0216	23.833	7.8	8	5.2	29	728.8	841.8	6.5662	0.0038	1.40	1.61
	TEST-4 RP9	6.4349	6.4296	-0.0053	0.0186	23.833	7.8	8	5.2	29	728.8	841.8	6.5662	0.0033	1.20	
	TEST-5 RP1	6.3351	6.3387	0.0036	0.0314	23.417	7.8	8	5.2	29	728.8	841.8	6.5662	0.0055	2.07	
	TEST-5 RP9	6.4121	6.4181	0.006	0.0268	23.417	7.8	8	5.2	29	728.8	841.8	6.5662	0.0047	1.76	
TN80SS	TEST-4 RP8	6.4884	6.4805	-0.0079	0.0224	23.833	7.8	8	5.2	29	728.8	841.8	6.5662	0.0039	1.45	1.61
	TEST-5 RP8	6.3786	6.3698	-0.0088	0.0268	23.417	7.8	8	5.2	29	728.8	841.8	6.5662	0.0047	1.76	
TN80Cr13	TEST-4 RP4	6.3255	6.3241	-0.0014	0.0023	23.833	7.8	8	5.2	29	728.8	841.8	6.5662	0.0004	0.15	0.17
	TEST-5 RP4	6.2929	6.2909	-0.002	0.0028	23.417	7.8	8	5.2	29	728.8	841.8	6.5662	0.0005	0.18	
TN110Cr13SS	TEST-4 RP3	6.2194	6.2196	0.0002	0.0004	23.833	7.8	8	5.2	29	728.8	841.8	6.5662	0.0001	0.03	0.03
	TEST-5 RP3	6.2714	6.2717	0.0003	0.0006	23.417	7.8	8	5.2	29	728.8	841.8	6.5662	0.0001	0.04	

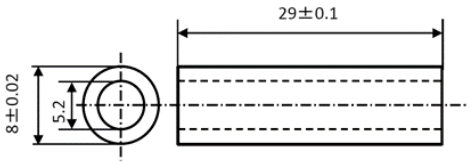

2016.2.3
☆Green columns are final Corrosion Rate.
☆Test TEST-4: 2015.11.4 9:10～2015.11.5 9:00 23h50min (23.833hr)
TEST-5: 2015.11.5 9:40～2015.11.6 9:05 23h25min (23.417hr)
☆Density
α-Fe:7.873(20℃)
It is used 7.8 in this analysis

Figure 19 Cylinder coupon after testing in Kakkonda

Table 5 Okuaizu1: Weight loss test using cylinder coupon

Material	Test ID	Initial Weight (g)	After Exposure (g)	Difference (g)	Difference After DHACP (g)	Exposure Time (h)	Specific Weight	O.D (mm)	I.D (mm)	Length (mm)	Area (mm2)	Volume (mm3)	Calculated Weight (g)	Corrosion Thickness (mm)	C.R. (mm/y)	C.R. Average (mm/y)
K-55	TEST -4 RP1	6.4577	6.4605	0.0028	0.0036	18.00	7.8	8	5.2	29	728.8	841.8	6.5662	0.0006	0.31	0.14
	TEST-4 RP11	7.0621	7.064	0.0019	0.0012	18.00	7.8	8	5.2	29	728.8	841.8	6.5662	0.0002	0.10	
	TEST-5 RP1	7.113	7.1157	0.0027	0.0013	19.65	7.8	8	5.2	29	728.8	841.8	6.5662	0.0002	0.10	
	TEST-5 RP11	6.855	6.857	0.002	0.0007	19.65	7.8	8	5.2	29	728.8	841.8	6.5662	0.0001	0.05	
TN80SS	TEST-4 RP8	6.9262	6.9284	0.0022	0.0014	18.00	7.8	8	5.2	29	728.8	841.8	6.5662	0.0002	0.12	0.10
	TEST-5 RP8	6.9556	6.958	0.0024	0.0011	19.65	7.8	8	5.2	29	728.8	841.8	6.5662	0.0002	0.09	
TN80Cr13	TEST-4 RP2	6.9172	6.9183	0.0011	0.0004	18.00	7.8	8	5.2	29	728.8	841.8	6.5662	0.0001	0.03	0.05
	TEST-5 RP2	6.8482	6.8494	0.0012	0.0008	19.65	7.8	8	5.2	29	728.8	841.8	6.5662	0.0001	0.06	
TN110Cr13SS	TEST-4 RP3	6.9736	6.9736	0	0.0009	18.00	7.8	8	5.2	29	728.8	841.8	6.5662	0.0002	0.08	0.07
	TEST-5 RP3	7.0637	7.0643	0.0006	0.0009	19.65	7.8	8	5.2	29	728.8	841.8	6.5662	0.0002	0.07	
SAF2507	TEST-4 RP4	6.8635	6.8634	-1E-04	0.0004	18.00	7.8	8	5.2	29	728.8	841.8	6.5662	0.0001	0.03	0.03
	TEST-5 RP4	7.0316	7.034	0.0024	0.0003	19.65	7.8	8	5.2	29	728.8	841.8	6.5662	0.0001	0.02	

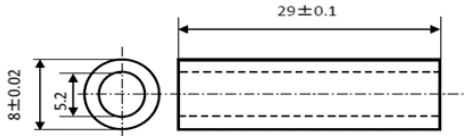

2016.2.10
☆ Green columns are final Corrosion Rate.
☆TEST TEST-4: 2016.1.27 15:15～2016.1.28 9:15 18h00min (18.000hr)
TEST-5: 2016.1.28 13:21～2016.1.29 9:00 19h39min (19.650hr)
☆Density
α-Fe:7.873(20℃)
It is used 7.8 in this analysis

2) Corrosion rate measured by weighing analysis were as follows. K-55, TN80SS: 1.61mm/year, TN80Cr13: 0.17mm/year, TN110Cr13S: 0.03mm/year
3) There was a difference of pitting rate between K-55, TN80SS and TN80Cr13, TN110Cr13S. The pitting rate of K-55, TN80SS were 7.7 ~20.8 mm/year and 2.5~7.6 mm/year for TN80Cr13, TN110Cr13S.
4) The corrosion rates estimated by Corrosometer® testing which were made using on-line results for apparent parabolic kinetics were 0.04~0.1mm/year. The

corrosion rate is one order of magnitude lower than for the weight loss analysis which assumes linear kinetics.

The results of Okuaizu1 field test are summarized as follows;

1) Result of Long Term Coupons; there is white deposit of K-55 and TN80SS. The white deposit also seen on TN80Cr13, but it was not so much. There was a red coloured area on TN80Cr13. There was no white deposit on TN110Cr13S, but the colour was slightly blue. It was thought that the colours were caused by thin oxide films on the material.
2) Result of SEM-EDS analysis; the white deposits were shown to be rich in Sb and As. The amount of the deposits was material dependant; K-55=TN80SS> TN80Cr13>TN110Cr13S>SAF2507.
3) Corrosion rate measured by weighing analysis were as follows: K-55, TN80SS: 0.1mm/year, TN80Cr13, TN110Cr13S, SAF2507: 0.03～0.07mm/year
4) There was some pitting on these materials; very few pits on TN110Cr13S and SAF2507. There was little difference of corrosion between TN80Cr13 and TN110Cr13S.
5) After testing, there were white and black adherent deposits on Corrosometer® CS probes. Analysis results of corrosion rate were quite low at 0.001~0.01mm /year. Analysis result of LPR testing, corrosion rate for K-55, TN80SS was 20μm/year, and 1.3μm/year for TN80Cr13 and 0.6μm/year for TN110Cr13S.

Okuaizu2 field test in 2017 was carried out to follow up Okuaizu1 field test in 2016. The objectives of this test were 1) Reliability study of short term test by comparison with long term test, 2) Examination in more extreme geothermal fluid environment by acid addition. In condition of the original geothermal fluid (pH3.8), we carried out the long term test for 15 days. By acid addition, we carried out on more acidic environment (pH3.0, H_2SO_4 or HCl). Table 6 gives results of these tests for carbon steel. Figure 20 shows corrosion rate measured by LPR for long term test (Test3, 15days). The corrosion rate of LPR was stabilized in a short period of time (approx.1000 minutes) while the corrosion rates from weight loss data of cylinder coupon and LPR probe electrode (TEST1, TEST2, TEST3) were also similar.

Regarding the detail of Okuaizu2 field test, please refer to our co-researchers' literature (Yanagisawa et al., 2017) on this proceeding.

Table 6 Okuaizu2: Field test results of Carbon steel

K-55 (Carbon Steel)

Test condition				Corrosion Rate			
TESTNo.	Condition	Exposure time	pH	Corrosometer (mm/y)	LPR (mm/y)	Weigt loss data Cylinder Coupon (mm/y)	Weigt loss data LPR Probe (mm/y)
TEST 1	Original Geothermal Fluid	1 day	3.8	0.001	0.029	0.191	0.181
TEST 2		4 days	3.8	0.0011	0.025	0.059	0.071
TEST 3		15 days	3.8	0.0047	0.046	0.064	0.086
TEST 4	add H_2SO_4	5.7 h	2.4	30	0.185	11.220	–
TEST 5	add H_2SO_4	20.7 h	3.0	5	0.061	0.690	13.827
TEST 7	add HCl	6.2 h	3.0	80	0.036	15.992	–

Figure 21 shows the pipe section profiling data of an injection pipeline of Kakkonda steam field in October 2016 and the pictures of open inspection at the plant maintenance. The profiling result (7mm thickness of scaling) is matching to the inspection result.

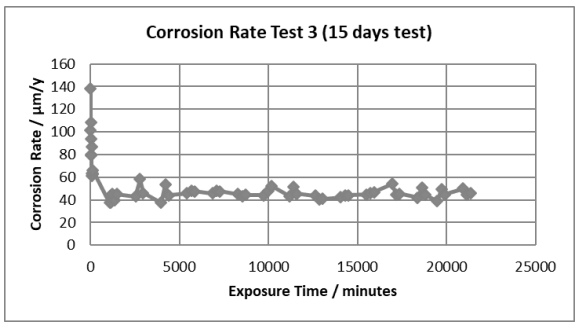

Figure 21 Okuaizu2: Corrosion rate of LPR (K-55(CS)) at TEST3 (15 days)

3.2 Gamma-ray pipe section profiler (GPSP)

In 2015 -2017, we have tried to apply GPSP in Kakkonda steam field (injection pipeline) and Okuaizu steam field (production pipeline) as given in Table 7 Figure 20 shows the pipe section profiling data of an injection pipeline of Kakkonda steam field in October 2016 and the pictures of open inspection at the plant maintenance. The profiling result (7mm thickness of scaling) is matching to the inspection result.

Table 7 Field tests in 2015 -2017

Field	M/Y (days)	Pipeline	Condition
Kakkonda	Nov.2015 Oct.2016	Injection (Liquid)	New piping Scaling
Okuaizu	Jan.2016	Production (2 phase)	Thin Scaling
	Nov.2016	Production (2 phase) with Neutralization	Thick Scaling
	Feb.2017		Thick Scaling
	Apr.2017		Thick Scaling

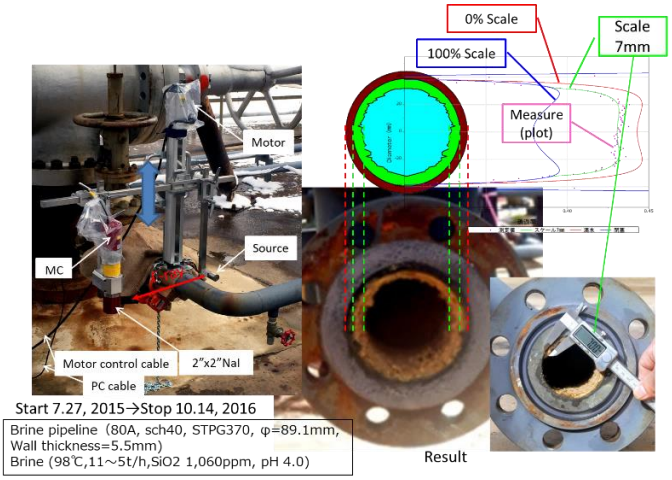

Figure 20 Pipe section profiling data and open inspection of the injection pipeline in Kakkonda

Figure 21 and 22 show the pipe section profiling data of a production pipeline (2 phase) of Okuaizu steam field during Jan.2016 to Apr.2017. This pipeline (400A) was being treated by neutralization using NaOH injection for acidity counter-measure of geothermal fluid. We started to measure before neutralization and monitored the scaling thickness change after neutralization at 330cm downstream from the NaOH injection port. Figure 21 shows comparison of scaling thickness during Jan.2016 to Apr.2017. After NaOH injection, we could find scaling but it was not changing during Nov. 2016 to Apr.2017. Therefore, we tried to measure additional 4 pipe sections (45cm, 78cm (covered by thermal insulator), 150cm (covered by thermal insulator), and 284cm) between

the injection port (0cm) and the monitoring point (330cm). Figure 22 shows 5 sections including the monitoring point. The scaling status of these 5 sections were different from profiling data of GPSP and more occluded between 78cm to 284cm because of turbulent flow and/or heterogeneous dispersion of injection NaOH. The scaling has not been found out at 45cm from the injection port since the port nozzle was located in central of the piping and the mixed fluid with NaOH did not get around to inner surface of the piping. We could measure in the same quality as in the case of piping without insulation material even when piping was covered with insulation material.

The pipeline opening inspections in Apr. 2017 showed more heterogenous scaling distribution but we could confirm the difference of scaling deposit at each piping section. GPSP system could not profile heterogeneous scaling distribution other than symmetrical shape or one side shape by reason of the fixed positioning of the source and the detector of GPSP. If the tool rotates or changes the position of source and detector, we can determine the heterogenous shape by tomographic theory. However, since our gamma-ray source is weak by limit of the regulation of treating radioactive source in Japan, we need approximately 4 hours (80A) to approximately 12 hours (400A) recording per one piping section profile. The tomographic technique would take a long time and would not be economical for industrial testing. Therefore, we focused to determine scaling blockage rate in piping section in short time for decision of maintenance timing. The system could work very well for this object.

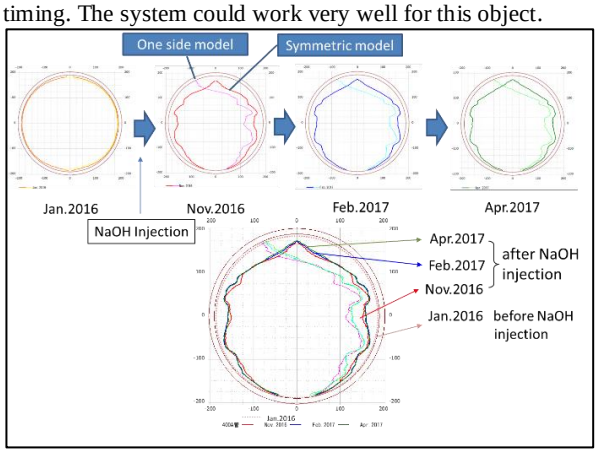

Figure 21 Scaling inspection of two phase production piping using GPSP in Okuaizu - Fixed point monitoring in Jan.2016 – Apr.2017

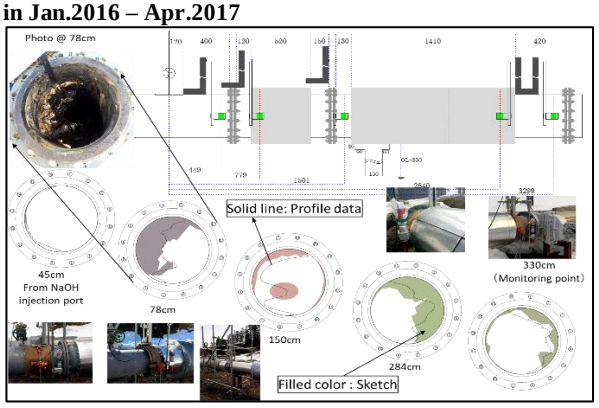

Figure 22 Scaling inspection of two phase production piping using GPSP in Okuaizu- Scale adhesion status on the downstream side of the Neutralization (NaOH) injection port with superposition of sketch at the pipeline opening inspections

4. CONCLUSION

We developed two new field testing tools for geothermal power plant risk assessment of corrosion and scaling. The first tool is the portable flow loop corrosion tester (PFCT) for more flexible and economical flow loop test in geothermal fields. The second tool is the gamma-ray pipe section profiler (GPSP) for more certain determination of pipeline clean-out schedule on plant maintenance. The two tools were tested in Kakkonda steam field and Okuaizu steam field in 2015-2017 and got good results. The next task of PFCT is how to determine reasonable corrosion rate in short time for corrosion control options such as corrosion inhibitors. The next task of GPSP is how to adapt tomographic technique for short time measurement to measure extreme heterogenous scaling in piping.

ACKNOWLEDGEMENTS

We thanks to Okuaizu Geothermal Co. Ltd. for the support of on-site test in Okuaizu steam field (Fukushima Prefecture) and Tohoku Sustainable & Renewable Energy Co. Inc. for the support of on-site test in Kakkonda steam field (Iwate Prefecture). This research project is supported by New Energy and Industrial Technology Development Organization (NEDO).

REFERENCES

Osato, K., Sato, M., and Kasai, K.: Coupled Analysis using 3D-CFD and Chemical Model for Corrosion and Scaling of Two Phase Flow Wellbore/Pipeline, Proc. 38th New Zealand Geothermal Workshop, Auckland, New Zealand (2016)

Lichti, K., White, S., and Sanada, N.: Modelling of Acid Fluid Wellbore Chemistry and Implications for Utilization. Proc. 20th New Zealand Geothermal Workshop, Auckland, New Zealand (1998), 103-108.

Lichti, K., White, S., and McGavin, P.: Software for Geothermal Corrosion and Risk Based Assessment, Proc. World Geothermal Congress 2005, Antalya, Turkey. (2005).

Rohrback Corroso Systems, Inc.: CORROSION MONITORING PRIMER, http://www.cosasco.com/documents/Corrosion_Monitoring_Primer.pdf, 61p.

Sanada, N., Kurata, Y., Nanjo, H., Kim, H., Ikeuchi, J. and Lichti, K., IEA Deep Geothermal Resources Subtask C: Materials, Progress with a Database for Materials Performance in Deep and Acidic Geothermal Wells, Proc World Geothermal Congress, Kyushu, Tohoku, Japan, (2000), 2411-2416.

Yanagisawa, N., Masuda, Y., Osato, K., Sato, M., Kasai, K., Sakura, k. and Fukui, T. : The estimation of the material corrosion based on previous data and compare with on-site test at geothermal field, Proc. 38th New Zealand Geothermal Workshop, Auckland, New Zealand. (2016)

Yanagisawa, N., Masuda, Y., Osato, K., Sato, M., Kasai, K., Sakura, K., Fukui, T., Akahorim M. and Lichti, K.: The Material Corrosion Test using Loop Sysytem under Acidic Condition at Geothermal Field in Japan, Proc. 39th New Zealand Geothermal Workshop, Auckland, New Zealand. (2017)